Design of HTS, Lumped-Element, Manifold-Type Microwave Multiplexers

George L. Matthaei, *Life Fellow, IEEE,* Stephan M. Rohlfing, and Roger J. Forse

Abstract—**Manifold-type frequency multiplexers are especially useful when a sizable number of channels are required. However, they normally use interconnecting transmission lines that could result in an overall structure many wavelengths across. Herein we investigate the design of compact manifold multiplexers using lumped-element filters which are convenient for high temperature superconductor (HTS) realization, while the transmission lines are replaced with lumped-element equivalents. Design examples calculated for frequencies in the vicinity of 0.8 GHz yield element values which are quite feasible for realization in HTS microstrip circuits. The examples indicate that very compact multiplexers should be obtainable.**

I. Introduction

WITH THE relatively recent strong interest in "wireless telecommunications" there is undoubtedly a need for frequency multiplexers operating in the vicinities of 0.8 and 2 GHz. A possible example might be the case of a wireless base station which has an antenna with transmitting and receiving equipment capable of covering a band of wireless frequencies, and the base station company sells transmission services for channels within its band. They might provide service to a number of independent operators that are licensed to operate in specific channels within the band covered by the base station. (The independent operators could be companies providing various types of communication service.) In order to separate out the various channels in the overall band transmitted and received by the base station, frequency multiplexers would be required. Another example of a possible need for multiplexers is the situation where a base station may wish to transmit various frequency channels in different directions by use of several directive antennas. In this case a multiplexer would be needed to separate the overall band transmitted by the base station into the channels which are to be radiated in the various directions. Doubtlessly similar types of situations exist in military communication systems.

Well developed techniques have been obtained for multiplexing a sizable number of channels for communication satellite systems. But those multiplexers are usually operating in the vicinity of X band or perhaps higher and may involve waveguide or other transmission-line structures that might be a number of wavelengths in size. If those techniques were utilized directly for design of multiplexers, for example, in the 0.8-GHz or 2-GHz range, the structure would be impractically large. Here we utilize some of the same principles that have been used for the satellite systems having, say, four or more channels, but we adapt them to use semi-lumped elements to give comparatively very small structures even when used at relatively low frequencies. The structures obtained are sufficiently small as to be of practical size for implementation in very-low-loss high-temperature superconductor (HTS) form which could greatly improve system performance.

The use of lumped-element techniques as described in this paper might also be of interest for use with normal metals for some situations. However, with the sizable number of elements required, and with the elements being realized in very compact microstrip form, the transmission loss would be quite large, especially since the filters used with manifold multiplexers are normally of relatively narrow bandwidth. In many systems this high loss would have to be compensated for by a large increase in costly transmitter power. (Higher transmitter power may also be objectionable for environmental reasons.) Another problem with a lossy normal-metal multiplexer circuit is that the shape of the passbands would be greatly distorted. If the filters were designed to have a flat Chebyshev passband the losses would distort the shape to be very rounded. There are "predistortion" design techniques for correcting for such response-shape distortions due to loss, but they would result in a design with even more flat loss, and the design process would be greatly complicated. Thus, the low losses obtainable using HTS could be very important in the design of compact multiplexers of the type discussed herein.

In the discussion above we have used examples related to the wireless frequency bands. However, the techniques discussed above may also be of great value for other frequencies also. A possible example might be, say, a complex S-band military airborne system requiring a number of multiplexers, each with a sizable number of channels. Further, the system might be desired to have the efficiency of waveguide systems while the total system must fit in a small space and be very light. The use of HTS along with the design approach described in this paper may provide means for meeting these extremely demanding objectives.

The design of microwave multiplexers poses some challenging problems, especially if the multiplexer is to be realized using high-temperature-superconductor (HTS) technology. One

Manuscript received October 13, 1995; revised February 12, 1996. This work was supported by the Naval Air Warfare Center, Warminster, PA, under Contract N62269-93-C-02233.

G. L. Matthaei is with Superconductor Technologies, Inc., Santa Barbara, CA 93111-2310 USA.

Stephan M. Rohlfing was with Superconductor Technologies, Inc., Santa Barbara, CA 93111-2310 USA. He is now with Rockwell International, Wireless Communications Division, Newbury Park, CA USA.

Roger J. Forse was with Superconductor Technologies, Inc., Santa Barbara, CA 93111-2310 USA. He is is now with Motorola, Schaumburg, IL USA.

Publisher Item Identifier S 0018-9480(96)04807-7.

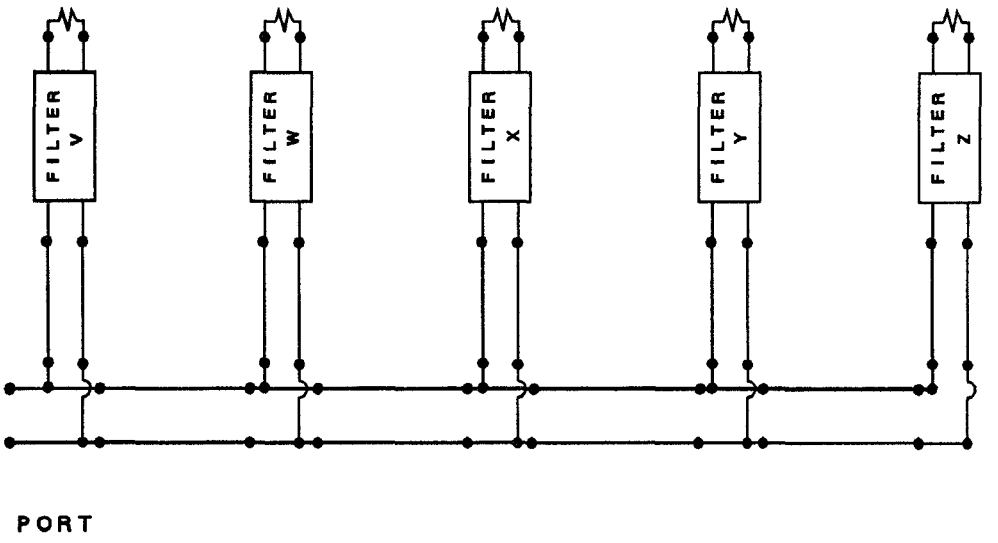

Fig. 1. A five-channel, manifold-type multiplexer. The lengths of the interconnecting transmission lines must be optimized.

problem arises from the fact that when a number of filters are interconnected so as to separate a given wide band of frequencies into a number of smaller channels, if the overall structure is not properly designed the filters will interact with each other so as to greatly degrade each other's performance. If the individual filters have cross-sectional dimensions at their inputs which are sufficiently small compared to a wavelength, there are relatively simple network synthesis methods that can be used for designing the channel filters so they will work well together if they are paralleled at a common interconnection point and a susceptance annulling network is added. (See Section 16.04 of [1].) It is often feasible to design multiplexers having two or three channels using this approach, and it is usually used for such situations. However, if more channels are required (especially if the channels are to be realized using waveguide filters), the input ports of the various filters will spatially interfere with each other if they are brought together to a common point, so this technique cannot be used.

For many present-day applications, such as communication satellites, multiplexers are needed with, perhaps, ten or more channels. For many of these applications "manifold" multiplexers are commonly used which have the individual channel filters mounted at intervals along a main transmission line (or manifold), as sketched in Fig. 1 for an example of a five-channel multiplexer. In many cases the manifold is made of waveguide. Manifold multiplexer structures have a major advantage in that a sizable number of filters can be interconnected, but their design is relatively involved. In order to obtain good results the interconnecting lines shown in Fig. 1 must have their lengths optimized, and the inputs to the various filters must also be optimized. In Fig. 1 the line lengths are all drawn as being more-or-less equal, whereas, actually, the lengths may vary considerably. On the average the lengths are of the order of a half wavelength. All of the filters and connecting lines interact with each other so that the optimization procedures needed to obtain good performance over the frequency range of all of the channels require a well-chosen strategy [2], [3]. It should also be recognized that since a manifold multiplexer involves many sizable lengths of transmission line and since the length of the manifold gets larger as more channels are added, the multiplexer bandwidth that is feasible becomes less as more channels are added. This is due to the increased frequency sensitivity of a longer manifold. Thus a manifold multiplexer with many channels is only feasible if the channels are relatively narrow band.

The use of manifold multiplexers for HTS technology introduces additional major considerations. Since the available sizes of substrates for materials such as $LaAlO_3$ and MgO, which are typically used for HTS circuits, is limited to around two or threef inches, it is not feasible to realize structures such as that in Fig. 1 using HTS since the overall structure is much too large. However, if the filters are realized in lumped-element form, and if the interconnecting transmission lines are replaced by lumped-element equivalents, then the realization of the structure using HTS looks much more attractive. In this work we investigate the practicality of HTS lumped-element multiplexers of this type.

II. Practical Lumped-Element HTS Bandpass Filters

Fig. 2 shows a seven-resonator, lumped-element bandpass filter of the type we have assumed in our trial multiplexer design. This type of bandpass filter is very attractive for narrow-band, HTS bandpass filter applications for a number of reasons. One is that the structure involves many degrees of freedom so that design parameters can be readily chosen to obtain element values of reasonable size. Note that the resonators in the structure each involve only one inductor and it is in series, and we can conveniently design the structure so that all of the inductors are the same. The dashed capacitors that bridge the inductors are only included if the inductor has parasitic capacitance that needs to be modeled as a capacitor in parallel with the inductor. For narrow-band filters the series capacitors (which are the resonator coupling capacitors) are quite small and easy to realize in microstrip, while the shunt capacitors are much larger but are also easy to realize.

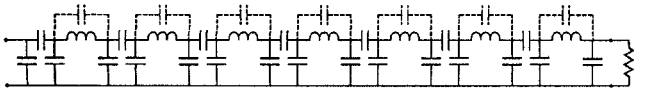

Fig. 2. A seven-resonator, lumped-element, bandpass filter of a type that is advantageous for use in HTS technology [5].

The element values for filters such as that in Fig. 2 can be obtained by use of filter synthesis programs such as SFILSYN [4]. However, the element values can also be obtained from lumped-element lowpass prototypes by adaptation of methods discussed in [1]. Using that approach, if for the moment we assume that the dashed capacitors in Fig. 2 are zero, the designer starts out with the bandpass filter [Fig. 8.02-3 of 1] with the resonators all consisting of an L and C in series, and with the resonators coupled by K inverters (i.e., impedance inverters). Each capacitor is replaced by two capacitors having twice the size, connected in series, one on each side of each inductor. Next the idealized K inverters are replaced by lumped-element equivalents of the form in Fig. 8.03-1(b) of [1]. In this way each inverter is replaced by a T network consisting of a positive shunt capacitance with a series negative capacitance on both sides. Then each series negative capacitance is merged with the adjacent positive, series, resonator capacitance to yield a net positive capacitance. At this point, the structure consists of series inductors separated by T configurations of capacitors. Application of T-to-pi transformations on the capacitors converts the structure to the form in Fig. 2, which has pi configurations of capacitors between the inductors. The circuitry at the ends of the filter can be modified using methods similar to those used in Section 8.11 of [1]. If it is desired to include parasitic capacitances such as the dashed capacitors in Fig. 2, they can be compensated for by including the parallel parasitic capacitor with each inductor and adjusting the resonator capacitor size in Fig. 8.02-3 of [1] to restore resonance at the desired center frequency. Then a corrected "reactance slope parameter" is computed for the resonators, and this slope parameter is used in computing the impedance inverter parameters from equations in Fig. 8.02-3 of [1]. The realization of circuits such as that in Fig. 2 in microstrip form was discussed in a previous paper [5].

III. Design of a Five-Channel Multiplexer Using Transmission Lines

It was decided to try a five-channel multiplexer example using seven-resonator, maximally flat channel filters of the form in Fig. 2. (Maximally flat rather than Chebyshev filters were used because a proposed application for this multiplexer called for reduced delay distortion.) The proposed example was to use channels with 3-dB bandwidths 20-MHz-wide, with the channel centers spaced 40 MHz apart, giving a 20 MHz guard band between channels. This gave a total overall bandwidth between the outer edges of the outer channels of 180 MHz. The multiplexer band was centered at 840 MHz giving an operating fractional bandwidth of 180/840 = 0.214.

The initial trial design was worked out using a transmission-line manifold configuration as in Fig. 1 which was designed by methods similar to those that have been used for waveguide multiplexers [2], [3]. This work was aided by helpful suggestions regarding the optimization process which were provided by Dr. Ali Atia.[1] The individual channel filters were designed from a lowpass prototype using techniques suggested in Section II above. For optimizing the interconnection of the filters to form a multiplexer as in Fig. 1, the line impedances were set at 50 ohms, and all of the transmission-line lengths were varied. In addition to optimizing the transmission-line lengths, for each channel filter the coupling at the input, the coupling between the first and second resonator, and the tuning of the first and second resonators were all varied in the optimization process.

From past experience with optimizing the design of individual bandpass filters we have found it to be insightful to use optimization parameters which independently vary specific resonator couplings without affecting the resonator tunings, and in some cases, independently vary the tunings of specific resonators without affecting the couplings. We decided to also apply that approach to the optimization of the input circuits of the channel filters in this multiplexer. Fig. 3 shows the first two resonators and their associated couplings for any of the channel filters. The elements in this figure that were varied are the capacitors CC01 to C12B, while elements C01A, C23, and CC23 were not varied (nor were the inductors or any of the other elements not shown which would be located to the right of this figure). The elements CC01, CC12, and CC23 are resonator coupling capacitors. Element scaling parameters $D01$ and $D12$ were introduced to vary the input coupling and the coupling between resonators 1 and 2. Scaling parameters $D1$ and $D2$ were introduced to vary the tuning of resonators 1 and 2, respectively. (All four parameters $D01$, $D12$, $D1$, and $D2$ were evaluated independently for each filter.) These parameters are set to one for no change in coupling or tuning, and are set to be greater or less than one to vary the coupling or tuning. The optimization was done using the Touchstone™ program [6] which has provision to introduce constraint equations among the circuit parameters. Constraint equations used, which permit the independent adjustment of resonator couplings and tunings for each filter, were:

$$\mathrm{CC01} = D01 * \mathrm{c01}, \tag{1a}$$

$$\mathrm{C01B} = \mathrm{c01B} - \frac{(D01 - 1) * \mathrm{cc01}}{2} + \frac{(D1 - 1) * \mathrm{c01B}}{2} \tag{1b}$$

$$C12A = c12A - (D12 - 1) * \mathrm{cc12} + \frac{(D1 - 1) * \mathrm{c01B}}{2} \tag{1c}$$

$$\mathrm{CC12} = D12 * \mathrm{cc12} \tag{1d}$$

and

$$C12B = c12B * D2 - (D12 - 1) * \mathrm{cc12}. \tag{1e}$$

In the above equations the capacitance values using lowercase c's refer to initial values of the capacitances in Fig. 3 as

[1] Private communication between G. L. Matthaei and A. E. Atia of CTA International.

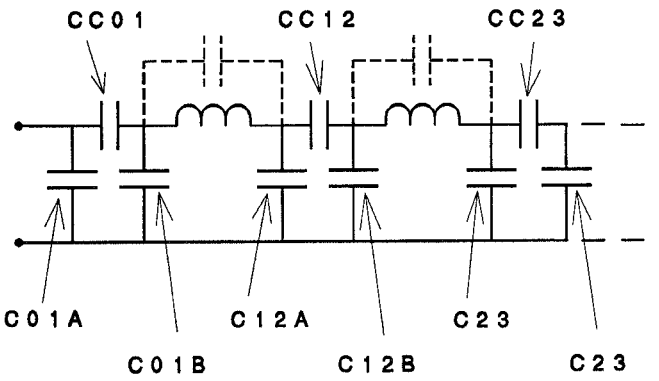

Fig. 3. The first two resonators of the filter in Fig. 2.

obtained by the methods of Section II, while the values using capital C's are the corresponding values after optimization. Of course, in the original Touchstone program additional identifiers were used to distinguish between the corresponding elements in the five different filters.

In the equations above, (1a) and (1d) relate to the adjustment of the coupling at the input of resonator 1 and the adjustment of the coupling between resonators 1 and 2, respectively. The second term on the right in (1c) and (1e) compensates for the change in the coupling capacitance CC12 so that this change will have no affect on the tuning of resonators 1 and 2. A precise tuning correction for a change in the coupling capacitor CC01 is much more complex, and for the present purposes only the very crude correction provided by the second term in (1b) was included. It was felt that since, herein, a separate tuning parameter for resonator 1 was also provided, a precise tuning correction for changes in CC01 was not very important. The third terms in (1b) and (1c), and the first term in (1e) relate to adjusting the tuning of resonators 1 and 2. Since the shunt capacitors in Fig. 3 are much larger than are the series coupling capacitors, small changes in the shunt capacitors for tuning have negligible affect on the coupling of resonator 1 to the input and the coupling between resonators 1 and 2.

With regard to the goals applied for the optimization process, goals were setup in view of the known, desired, maximally flat response for each filter. For each channel a goal of 24.5 dB attenuation at plus and minus 15 MHz from channel center was specified, along with a goal of 3 dB attenuation at plus or minus 10 MHz from the channel center frequency, and a goal of having in excess of 34 dB return loss throughout a 12 MHz band at the center of each channel. (Since the filters are maximally flat, ideally, the return loss for each filter should become infinite at the center of each channel.)

For the optimization, all of the line lengths were initially set to a half wavelength at 840 MHz, and adjustment parameters were used to scale them individually from that length. Also, all of the filter elements were set to their initial values as obtained in Section II above. It is important not to attempt to vary all of the parameters at once as this may cause the optimizer to hang up on a local minimum. We started out by varying only the line lengths while keeping the filter elements fixed. Then the line lengths were held fixed while the filter elements discussed above were varied. Next the lumped elements and input line for the channel with the poorest response were optimized. Then we moved on to the next poorest channel, etc. Later the manifold lines were re-optimized, etc. In time quite good overall responses were obtained which were similar to those in Fig. 6 (which are for the lumped-element manifold structure to be discussed in the next section).

It is of interest to note the line lengths that were obtained from the optimization process. Starting from the common port on the left in Fig. 1 the lengths of the sections of the main line of the manifold are 0.937, 1.400, 1.176, and 0.441, all measured in half wavelengths at fo = 840 MHz. Similarly the input lines to the channel filters are, starting with Channel V, 0.287, 0.05, 0.786, 0.586, and 0.646, again all measured in half wavelengths at fo. (Note that the second line is so short that it will not need to be replaced by a lumped equivalent.) As previously mentioned, these lines are all of 50-ohms impedance. Clearly, if we were to attempt to realize this structure using these transmission lines it would be much too large to be practical for use with HTS technology.

IV. Design of a Five-Channel Lumped-Element Multiplexer

Now we shall wish to replace each length of transmission line in the structure in Fig. 1 by a lumped-element equivalent consisting of a pi section, or a cascade of pi sections, where each pi section consists of a series inductance L with a shunt capacitance C on each side. For a single frequency we could replace any of the line sections by a single pi section; however, since we want the lumped-element structures to model the transmission-line structures over a 21% bandwidth, we will need to cascade several pi sections to get a reasonable approximation for the longer line lengths over the required bandwidth.

In order to relate a pi section to a corresponding length of transmission line it is convenient to analyze the pi section in terms of its image parameters. (See Section 3.02 of [1].) The image impedance Zi of a pi section consisting of a series inductor L with a shunt capacitor C on each side is

$$Zi = \sqrt{\frac{L}{2C}} \frac{1}{\sqrt{1 - \left(\frac{\omega}{\omega_c}\right)^2}} \tag{2}$$

where

$$\omega_c = \sqrt{\frac{2}{LC}} \tag{3}$$

is the lowpass cutoff frequency of the pi section in radians/sec. The image phase shift of the pi section is

$$\phi = 2 \sin^{-1}\left(\frac{\omega}{\omega_c}\right). \tag{4}$$

In order to replace a length of transmission line by a pi section that is electrically equivalent at a given frequency fo, we design the pi section so that at frequency fo the image impedance Zi in (2) equals the characteristic impedance of

the transmission line, and ϕ in (4) equals the phase shift of the transmission line at fo.

In order to design a pi section to replace a given length of transmission line at a given frequency fo it is convenient to define the length of the transmission line in terms of half wavelengths at frequency fo. We will use S to symbolize this normalized length where

$$S = \frac{2fo\,d\sqrt{\varepsilon_{eff}}}{c_o} \tag{5}$$

d is the physical length of the transmission line, ε_{eff} is the effective dielectric constant for propagation on the transmission line, and c_o is the velocity of light in a vacuum. Using (2)–(5), in order to get the L and C values for a pi section so as to have at fo a desired image impedance Zi and a phase shift corresponding to S half wavelengths of transmission line, we obtain

$$L = \frac{Zi\ 2\sin\left(\frac{\pi S}{2}\right)\sqrt{1-\sin\left(\frac{\pi S}{2}\right)^2}}{2\pi fo} \tag{6}$$

and

$$C = \frac{\sin\left(\frac{\pi S}{2}\right)}{Zi\ 2\pi fo\sqrt{1-\sin\left(\frac{\pi S}{2}\right)^2}}. \tag{7}$$

By use of these equations the plots in Fig. 4(a) were prepared where L in nh and C in pf are plotted versus S in half wavelengths for the case of $Zi = 50$ ohms and $fo = 0.840$ GHz as for our trial multiplexer design. It is interesting to note that due to the cutoff characteristic of the pi section, for S larger than 0.5 the value of L required decreases for increasing S. Actually, because of the rapidly increasing frequency sensitivity of the resulting pi section as S is increased, in most situations one would probably not wish to use an S much larger than 0.5 and for many situations a considerably smaller value may be preferable. To achieve this it may be necessary to model the transmission line using a cascade of two or more pi sections.

In order to obtain a better picture of the frequency sensitivity of pi sections the plots in Fig. 4(b) were prepared. The upper curve shows dZi/df, the rate of change of the image impedance with frequency, where here f is in GHz. The derivative is evaluated at $fo = 0.840$ GHz for $Zi = 50$ ohms at fo. Note that the derivative increases rapidly as S is increased. The lower curve is an analogous plot for $d\Delta\phi/df$ in degrees per GHz where $\Delta\phi$ is the deviation of the phase of the pi section from the phase of the transmission-line section being modeled. From this it is clear that at frequencies off of fo the difference between the phase of the pi section and that of the transmission line will increase rapidly as S is increased.

Though it was planned to re-optimize the circuit after the transmission lines are replaced by lumped-element equivalents, it was felt that the design would probably go more smoothly if, at least for the main lines in the manifold (i.e., the horizontally oriented lines in Fig. 1), the deviations of the electrical characteristics of the lumped-element circuits from those of the corresponding transmission-line sections are kept reasonably small over the frequency band of interest. For this reason most of the main lines were divided into two or

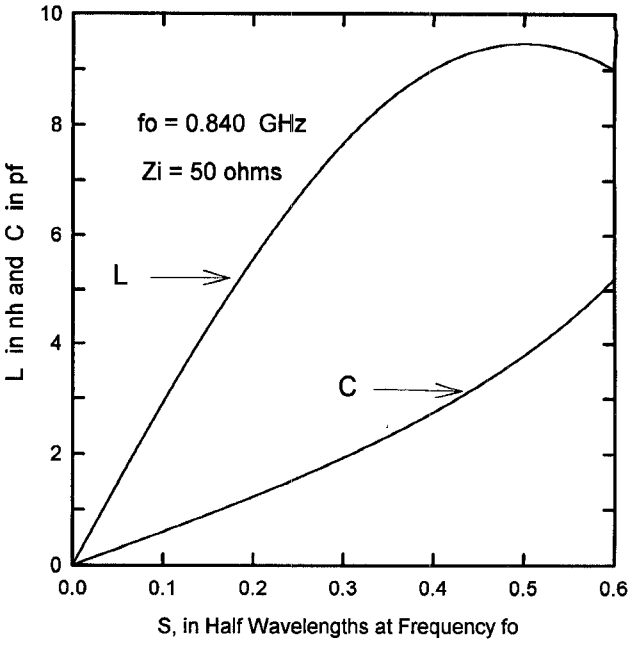

(a)

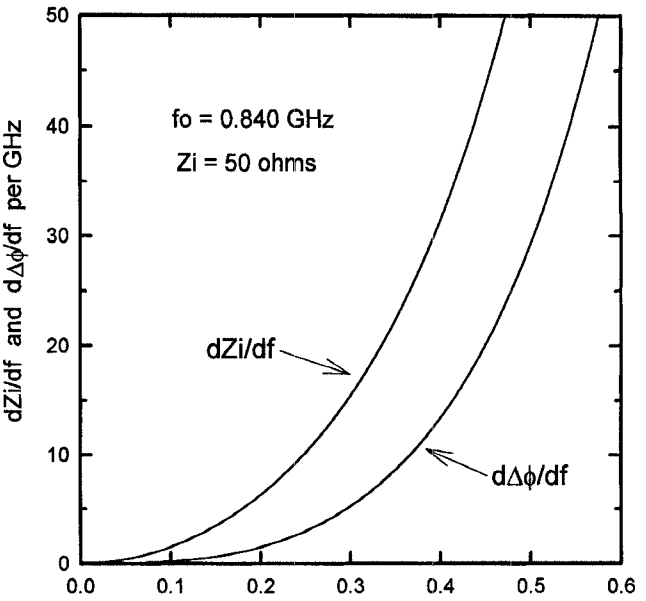

(b)

Fig. 4. (a) The inductance L in nh and capacitance C in pf for a pi section that models a 50-ohm transmission line which is S half-wavelengths long at $fo = 0.840$ GHz. The pi section consists of a series inductor L with a shunt capacitor C on both sides. (b) The dZi/df curve is the rate of change of the image impedance versus frequency for the pi section in Fig. 4(a) plotted against the electrical length S at frequency fo of the corresponding transmission line. The $d\Delta\phi/df$ curve is defined analogously, where $\Delta\phi$ is the difference between the phase shift of the pi section and the phase shift of the corresponding transmission line.

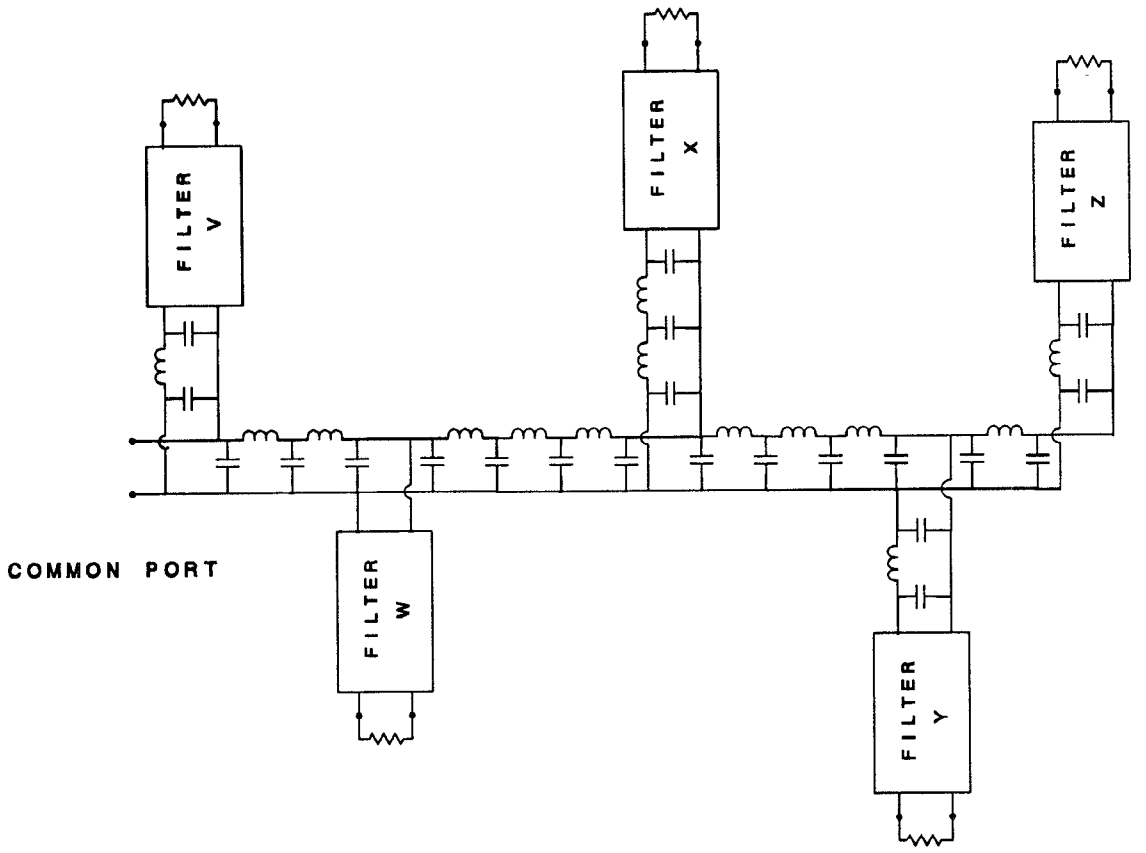

Fig. 5. A five-channel multiplexer analogous to that in Fig. 1 except that the transmission lines have been replaced by lumped-element artificial transmission lines. The filter circuits are of the form in Fig. 2.

three equal subsections, and each subsection was individually modeled by a pi section. The largest value of S used for any of these main-line subsections was 0.469 half wavelengths at fo. Using this value of S the image impedance of the pi section deviates from 50 ohms by -5.29 ohms at 0.70 GHz and by $+6.94$ ohms at 0.95 GHz. Meanwhile the phase deviates from that of an ideal transmission line by -2.25 degrees at 0.70 GHz and by $+3.4$ degrees at 0.95 GHz. In this particular case two subsections were used, and, since the phase errors of the individual subsections are additive, the overall phase errors for the two pi sections in cascade are -4.40 degrees at 0.70 GHz and 6.8 degrees at 0.95 GHz. Note that, no matter how many subsections are used, the image impedance for the cascade of pi sections is still the same (see Section 3.02 of [1]) so the impedance errors for the two subsections in cascade are the same as for a single section. It is of interest to note that when two or more pi sections are connected in cascade, at the points where two pi sections interface with each other there are two capacitors in parallel so the total capacitance is $2C$, while at the ends of the cascade of pi sections the capacitor values will be simply C.

It was felt that for the line sections which connect individual filters to the main line (i.e., the vertically oriented lines in Fig. 1), keeping the errors due to frequency sensitivity low would be less critical since these line lengths are highly sensitive mainly in the relatively narrow passband of the filter to which the line is connected. For that reason we modeled the 0.586-half-wavelengths-long line at the input to channel filter Y by a single pi section. For this pi section, the impedance and phase deviations are, respectively, -10.87 ohms and -5.33 degrees at 0.7 GHz and 9.13 ohms and 4.57 degrees at 0.95 GHz. At the input to channel filter W the required line length was only 0.05 half wavelengths so this was realized as an actual transmission line. After all the transmission lines were modeled by one or more pi sections, the circuit in Fig. 1 looked as shown in Fig. 5.

The performance of the circuit shown in Fig. 5 with the element values for the lumped-element interconnecting circuits determined as outlined above was similar to that of the original circuit as shown in Fig. 1 except that the performance in the individual passbands was somewhat degraded. It was decided to re-optimize to correct for this. A number of strategies for re-optimization could have been used. For example, it would have been feasible to utilize constraint equations that would guarantee that the image impedance of all of the pi sections was held at 50 ohms at frequency fo while the phase of the pi sections was allowed to vary. (This would have been analogous to what was done in the optimization for the circuit in Fig. 1.) However, what we decided to try was to allow the L and C for each set of pi sections to vary. In addition, where there is a T junction having two or three shunt capacitors in parallel we merged these capacitors together and optimized the resulting total capacitance. The couplings and resonator tunings for the first two resonators of each filter were also allowed to vary, as

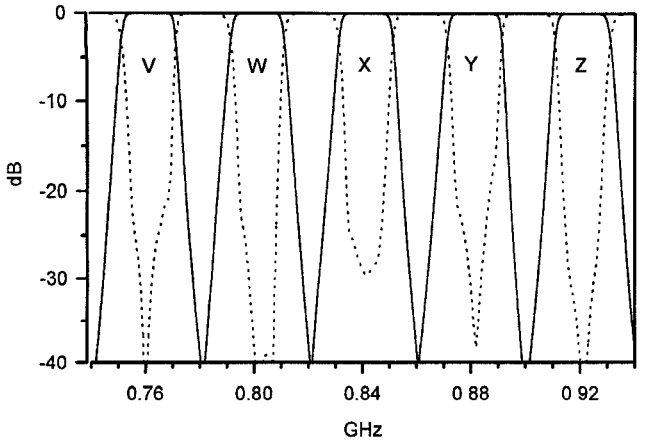

Fig. 6. The computed responses for the multiplexer in Fig. 5. The solid lines show the transmission characteristics from the common input port to the outputs of the various filters. The dashed lines show the return loss seen at the common port.

was discussed in Section III above. The computed results for the final design are shown in Fig. 6. The performance achieved is well within the design objectives.

V. A Two-Channel Design for Detailed Evaluation

It was desired to work out more completely the design of a simple multiplexer to verify that its physical dimensions are reasonable, to clarify what a practical physical layout would be, and to be available to fabricate at some later date. The five-channel design in Fig. 5 seemed overly complex for an initial trial structure, so it was decided to obtain a two-channel design for this purpose. In this design we used only the Channel V and Channel W filters, and carried out the design process as before. The resulting circuit is shown in Fig. 7, and its computed response is shown in Fig. 8. Again the performance satisfies the proposed design objectives quite well.

Considerable thought was given to the matter of how the manifold structure can be realized in microstrip using a configuration that can readily be adapted for use with multiplexers having more channels. It was assumed that the substrate would be 0.273-mm-thick lanthanum aluminate ($LaAlO_3$) having a relative dielectric constant of $\varepsilon_r = 23.5$. The resulting microstrip layout of the manifold structure is shown in Fig. 9. The details of how the design dimensions for this structure were obtained were discussed in a previous paper [7]. A point of interest from that paper is that the accuracy of modeling the two-port shunt capacitances (which are the rectangular-pad areas in Fig. 9) over the desired band of frequencies is enhanced if the ratio of length to width of these capacitor pads is properly chosen. In particular, the capacitors were modeled by a T equivalent consisting of a shunt capacitance with a small series inductance on both sides. If the proportions of the capacitor pad are chosen optimally the values of the elements in the circuit will be virtually independent of frequency, but the shunt capacitance tended to vary some with frequency for other proportions. (The equivalent-circuit element values were determined over the frequency band using a full-wave field solver [8].) Similarly, it was found that for the case of three-port capacitors the modeling over a band of frequencies

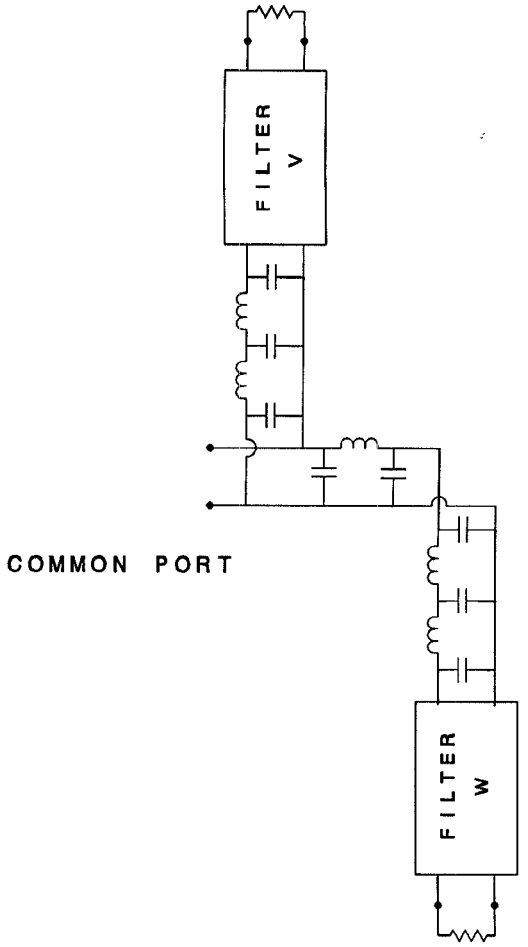

Fig. 7. The circuit diagram for a 2-channel manifold-type multiplexer using artificial transmission lines. Again, the filter circuits are of the form in Fig. 2.

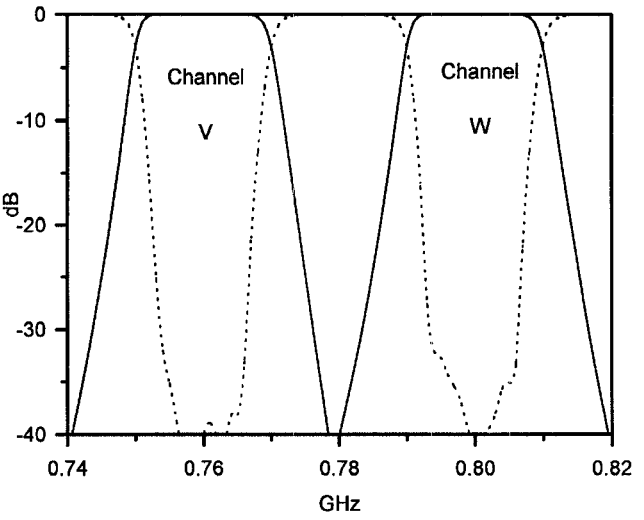

Fig. 8. The computed responses for the two-channel multiplexer in Fig. 7. As in Fig. 6 the solid lines show the transmission characteristics through the two channels while the dashed lines show the return loss seen at the common port.

is improved if the capacitors are of hexagonal shape, as shown in Fig. 9. This is because the symmetry of the hexagon lends itself to an equivalent circuit with a shunt capacitor

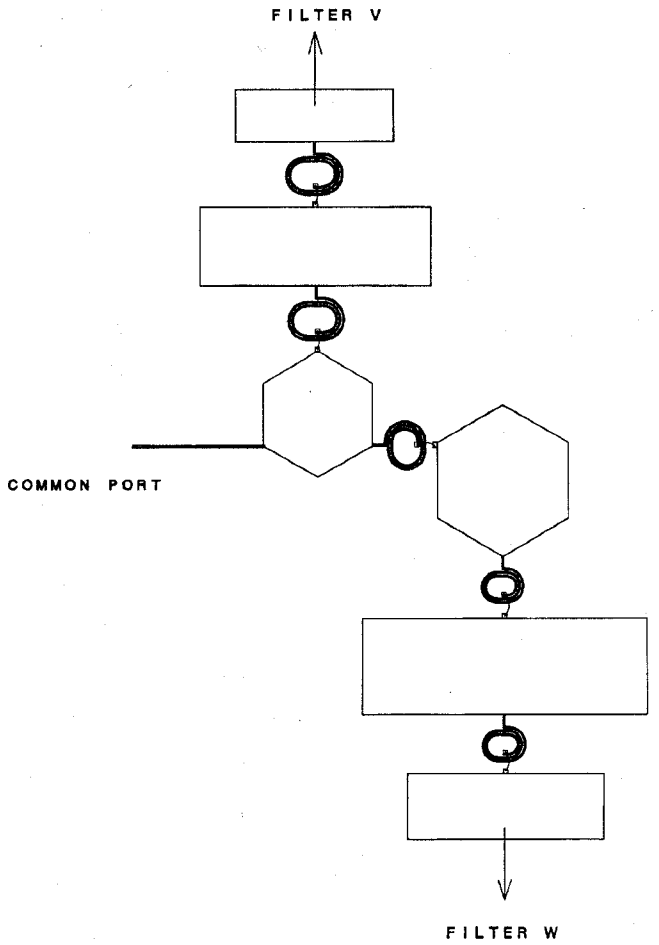

Fig. 9. A proposed microstrip realization of the lumped-element, artificial-transmission-line structure in the manifold-type, two-channel multiplexer in Fig. 7. The rectangular and hexagonal regions are shunt capacitors while the ovals are spiral inductors.

with a small, series inductor connecting to each of the three ports. The series inductors in these equivalent circuits can be compensated for by a small reduction in the size of the adjacent series inductors called for in the circuit. The general approach used for design of the spiral inductors in Fig. 9 is also briefly discussed in [7].

The dimensions for the structure in Fig. 9 appear to be very reasonable. The distance from the upper side of the rectangular capacitor at the top to the lower side of the rectangular capacitor at the bottom is about 16.8 mm. A multiplexer with more channels can be laid out in a similar manner with the locations of the filters extending to the right and alternating between the top and bottom of the manifold as suggested in Fig. 5. It would probably be convenient to fabricate the manifold on one substrate and each individual filter on a separate substrate. If the joints between substrates are placed at inductor bond wires the joints may have little electrical effect.

VI. Conclusion

This study has provided means for obtaining manifold multiplexer designs using lumped elements instead of lengthy transmission lines. The proposed design procedure for getting the circuit elements was found to work quite well, and the trial design in the 0.800 GHz range was found to have quite reasonable circuit element values for realization in microstrip. On the basis of the fact that one of our previous seven-resonator, HTS bandpass filters of the type in Fig. 2 for the 0.8-GHz frequency range used a $LaAlO_3$ substrate about 25 × 10 mm, and from our calculations for the circuit in Fig. 9, we estimate that using $LaAlO_3$ substrates a realization of the five-channel design in Fig. 5 might span an area of about 51 × 64 mm (2 × 2.5 inches). This covers the extent of the substrates but does not include the additional space required for a housing and connectors. As discussed previously, we believe that the circuit would not need to be all placed on a single substrate, but instead could be pieced together using several substrates with the joints between substrates being where bond wires cross to inductors.

The results of the designs carried out in this work suggest that the techniques herein should be feasible for applications such as the examples discussed in the Introduction to this paper.

References

[1] G. L. Matthaei, L. Young, and E. M. T. Jones, *Microwave Filters, Impedance-Matching Networks, and Coupling Structures.* Norwood, MA: Artech, 1980.
[2] A. E. Atia, "Computer-aided design of waveguide multiplexers," *IEEE Trans. Microwave Theory Tech.*, vol. 22, pp. 332–336, Mar. 1974.
[3] X.-P. Liang, K. A. Zaki, and A. E. Atia, "Channel expansion and tolerance analysis of waveguide manifold multiplexers," *IEEE Trans. Microwave Theory Tech.*, vol. 40, pp. 1591–1594, July 1992.
[4] SFILSYN computer program, DGS Associates, Santa Clara, CA.
[5] D. G. Swanson, R. Forse, and B. J. L. Nilsson, "A 10 GHz thin film lumped element high temperature superconductor filter," in *1992 IEEE MTT-S Intl. Microwave Symp. Dig.*, Piscataway, NJ, pp. 1191–1193.
[6] Touchstone™ computer program, HP EEsof, Westlake Village, CA.
[7] G. L. Matthaei and R. J. Forse, "A note concerning the use of field solvers for the design of microstrip shunt capacitances in lowpass structures," *Int. J. Microwave and Millimeter-Wave Computer-Aided Eng.*, vol. 5, pp. 352–358, 1995.
[8] EM, a full-wave field solver program for planar circuits. The program is produced by Sonnet Software, Suite 100, 101 Old Cove Road, Liverpool, NY.

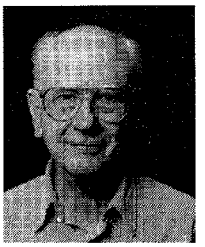

George L. Matthaei (S'49–M'57–F'65–LF'89) received the B.S. degree from the University of Washington, Seattle, in 1948, and the Ph.D. degree from Stanford University, Stanford, CA, in 1952.

From 1951 to 1955, he was on the faculty of the University of California, Berkeley, where he was an Assistant Professor, and his specialty was network synthesis. From 1955 to 1958, he was engaged in system analysis and microwave component research at the Ramo-Wooldridge Corporation. From 1958 to 1964, he was at the Stanford Research Institute, where he was engaged in microwave device research and became Manager of the Electromagnetic Techniques Laboratory in 1962. In July 1964, he joined the Department of Electrical Engineering, University of California, Santa Barbara, where he was a Professor. He retired in July 1991 and became a Professor Emeritus. At that time, he joined the staff of Superconductor Technologies, Inc., Santa Barbara, part time. He is the author of numerous papers, co-author of the book *Microwave Filters, Impedance-Matching Networks, and Coupling Structures*, and a contributor to several other books. His current interests are in the area of the application of high-temperature superconductivity to passive and active microwave and millimeter-wave circuits.

Dr. Matthaei is a member of Tau Beta Pi, Sigma Xi, and Eta Kappa Nu. He was the winner of the 1961 Microwave Prize of the IEEE MTT Group. In 1984, he received the IEEE Centennial Medal and in 1986 the Microwave Career Award of the IEEE Microwave Theory and Techniques Society.

Stephan M. Rohlfing received the B.S.E.E. degree from the Stevens Institute of Technology, Hoboken, NJ, in 1984.

From 1984 to 1988, he worked for the Microwave Semiconductor Corp., Somerset, NJ, designing both hybrid and discrete amplifiers. He was then with Veritech Microwave, South Plainfield, NJ, before joining Amplica, Inc., Newbury Park, CA, in 1988, where he designed hybrid amplifiers. In 1991, he joined Superconductor Technologies, Santa Barbara, CA, doing research and development on HTS filters. In January 1996, he joined Rockwell International, Wireless Communications Division, Newbury Park, to design MMIC's.

Roger J. Forse received the B.S.E.E. and M.S.E.E. degrees from the University of Illinois, Urbana, in 1970 and 1975, respectively.

He designed thin film receiver subsystems at Watkins-Johnson and Avantek from 1975 to 1990. In 1990, he joined Superconductor Technologies, Inc., Santa Barbara, CA, where he worked on HTS filter design. At the end of 1995, he joined Motorola, Schaumburg, IL, where he is working on the modeling of RF printed circuits.